



3D characterization of partially recrystallized Al using high resolution diffraction contrast tomography

Sun, Jun; Yu, Tianbo; Xu, Chaoling; Ludwig, Wolfgang; Zhang, Yubin

Published in:
Scripta Materialia

Link to article, DOI:
[10.1016/j.scriptamat.2018.08.001](https://doi.org/10.1016/j.scriptamat.2018.08.001)

Publication date:
2018

Document Version
Peer reviewed version

[Link back to DTU Orbit](#)

Citation (APA):
Sun, J., Yu, T., Xu, C., Ludwig, W., & Zhang, Y. (2018). 3D characterization of partially recrystallized Al using high resolution diffraction contrast tomography. *Scripta Materialia*, 157, 72-75.
<https://doi.org/10.1016/j.scriptamat.2018.08.001>

General rights

Copyright and moral rights for the publications made accessible in the public portal are retained by the authors and/or other copyright owners and it is a condition of accessing publications that users recognise and abide by the legal requirements associated with these rights.

- Users may download and print one copy of any publication from the public portal for the purpose of private study or research.
- You may not further distribute the material or use it for any profit-making activity or commercial gain
- You may freely distribute the URL identifying the publication in the public portal

If you believe that this document breaches copyright please contact us providing details, and we will remove access to the work immediately and investigate your claim.

Manuscript Number: SMM-18-1215R1

Title: 3D characterization of partially recrystallized Al using high resolution diffraction contrast tomography

Article Type: Regular article

Keywords: recrystallization; 3D reconstruction; Schwartz-Saltykov analysis; electron backscattering diffraction (EBSD); aluminium

Corresponding Author: Dr. Yubin Zhang, Ph.D

Corresponding Author's Institution: Technical University of Denmark

First Author: Jun Sun

Order of Authors: Jun Sun; Tianbo Yu; Chaoling Xu; Wolfgang Ludwig; Yubin Zhang, Ph.D

Abstract: Synchrotron diffraction contrast tomography (DCT) is for the first time used to characterize recrystallized grains in partially recrystallized Al. The positions, orientations and 3D shapes of more than 900 recrystallized grains are reconstructed within a gauge volume. The results are compared with those obtained using electron backscattered diffraction based on a statistical analysis. It is found that recrystallized grains with size larger than 10 μm , corresponding to ~98% of the total recrystallized volume of the sample, are well characterized by DCT. The advantages of DCT for recrystallization studies and new possibilities with DCT on new generation synchrotron sources are discussed.

3D characterization of partially recrystallized Al using high resolution diffraction contrast tomography

Jun Sun^{1,2}, Tianbo Yu¹, Chaoling Xu³, Wolfgang Ludwig^{4,5}, Yubin Zhang^{1*}

¹ Department of Mechanical Engineering, Technical University of Denmark, 2800 Kgs. Lyngby, Denmark.

² Xnovo Technology, 4600 Køge, Denmark

³ Department of Management and Engineering, Linköping University, SE-58183 Linköping, Sweden

⁴ ESRF, 6 rue Jules Horowitz, Grenoble 38043, France.

⁵ University of Lyon, MATEIS, INSA-Lyon, UMR 5510 CNRS, 7 Avenue Jean Capelle, Villeurbanne 69621, France.

* Email address: yubz@mek.dtu.dk; postal address: Technical University of Denmark, Produktionstorvet, Building 425, room 214, 2800 Kgs. Lyngby, Denmark. Phone: +45 45254752.

Abstract:

Synchrotron diffraction contrast tomography (DCT) is for the first time used to characterize recrystallized grains in partially recrystallized Al. The positions, orientations and 3D shapes of more than 900 recrystallized grains are reconstructed within a gauge volume. The results are compared with those obtained using electron backscattered diffraction based on a statistical analysis. It is found that recrystallized grains with size larger than 10 μm , corresponding to ~98% of the total recrystallized volume of the sample, are well characterized by DCT. The advantages of DCT for recrystallization studies and new possibilities with DCT on new generation synchrotron sources are discussed.

Keywords: recrystallization; 3D reconstruction; Schwartz-Saltykov analysis; electron backscattering diffraction (EBSD); aluminium

During recrystallization of deformed materials, nearly defect-free nuclei/grains form and grow at the expense of the surrounding deformed matrix. Recent 3D results obtained using serial sectioning have shown that the distribution of nuclei/recrystallized grains is heterogeneous non-uniform, and depends strongly on the local deformation microstructure [1–4]. Although both deformed matrix and nuclei/recrystallized grains can be characterized with these techniques, only limited volume or limited spatial resolution can be obtained when the sectioning is done with focused ion beam [1] or mechanical polishing [2–4], respectively. More importantly, the destructive nature of the techniques prohibits the possibility of dynamic studies to follow the recrystallization process, which is essential for a better understanding of the heterogeneities of recrystallization.

During the last 15-20 years, several non-destructive 3D characterization techniques have been invented and implemented using synchrotron X-rays, including 3D X-ray diffraction (3DXRD) [5–8], diffraction contrast tomography (DCT) [9,10], Bragg coherent diffraction imaging [11,12] and 3D X-ray Laue microdiffraction [13,14]. Among these techniques, DCT allows fast 3D reconstruction of grains in fully recrystallized samples [15,16]. Although the nuclei/grains in partially recrystallized samples are also in the recrystallized state (i.e. with very low densities of interior defects), the nuclei/grains are relatively small compared to those in fully recrystallized samples. At the same time, parts of the microstructure consist of deformed grains with significant orientation variations and strain gradients. Some of the nuclei/grains may have orientations similar to the neighboring deformation grains, from which they originate. All these factors make reconstruction of the recrystallized

1 grain very challenging [10]. To what extent DCT can be used to characterize partially
2 recrystallized samples is therefore still an open question.
3

4 In the present paper, we will for the first time explore the applicability of DCT
5 for recrystallization characterization. A partially recrystallized Al sample will be used
6 as a model material. To validate the DCT results, they will be compared with those
7 obtained based on conventional characterization using electron backscattered
8 diffraction (EBSD). Statistical analysis will be performed to link the 2D EBSD and
9 the 3D DCT results and ease the interpretation of the results.
10
11
12
13
14
15
16
17
18

19 Commercial purity aluminium, Al1050, was used for the present study. The
20 starting material had a fully recrystallized microstructure with an average grain size of
21 ~50 μm . The material was then cold rolled to 50% reduction in thickness, followed
22 by annealing at 325 °C for 0.5 h to obtain a partially recrystallized microstructure. For
23 the synchrotron DCT measurement, pillar samples with cross-section of $\sim 420 \times 420$
24 μm^2 were cut out using electrical discharge machining. The DCT measurement was
25 conducted at beamline ID11 at the European Synchrotron Radiation Facility (ESRF).
26 The X-ray energy was 37 keV. The direct X-ray beam was constrained by two sets of
27 vertical and horizontal slits to $240 \times 420 \mu\text{m}^2$. Transfocators with beryllium lenses
28 were used to focus the beam. A uniform beam was obtained within the defined gauge.
29 The sample was mounted on an ω rotation stage with the sample rolling direction
30 (RD) parallel to the vertical rotation axis. A full 360° scan was performed with
31 angular integration steps of 0.1° and an exposure time of 2 s. Both the diffracted and
32 the transmitted beam were recorded using a near-field detector (comprising a
33 transparent luminescent screen, light optically coupled to a CCD) with 2048×2048
34 pixels positioned normal to the incident beam at a sample-to-detector distance of 3
35 mm. To improve the spatial resolution, an eyepiece was used to magnify the
36
37
38
39
40
41
42
43
44
45
46
47
48
49
50
51
52
53
54
55
56
57
58
59
60
61
62
63
64
65

1 | diffraction images. The effective pixel size of the detector system was 0.77 μm . The
2 | detailed information about the DCT setup can be found in [9,10].
3 |

4 | A typical diffraction image is shown in Fig. 1. Most of the diffraction spots,
5 | e.g. those marked by the red arrows, are sharp and well-defined, appearing typically at
6 | 1-2 consecutive angular steps. These diffraction spots originate from recrystallized
7 | grains. Only few blurry, large and weak diffraction spots, as the one marked by the
8 | yellow ellipse, are visible and appear typically over a large number of angular steps.
9 | These originate from the deformed matrix.
10 |

11 | The diffraction images were analyzed with the DCT software
12 | (<http://sourceforge.net/projects/dct>) available at the beamline. A recently developed
13 | algorithm allowing 6D reconstruction (3D for position + 3D for orientation) [17,18] is
14 | used to reconstruct the grain shapes. In total 929 recrystallized grains are found within
15 | the gauge volume. The 3D volume is shown in Fig. 2a. The recrystallized grains are
16 | typically not spherical but elongated along the RD and the transverse direction (TD).
17 | Also the recrystallized grains are not randomly distributed, but clustered in bands
18 | parallel to the RD and TD. For clear visualization, a typical 2D section is shown in
19 | Fig. 2b. The volume fraction, V_V , of the recrystallized grains is about 24% and the
20 | average grain size (defined as equivalent spherical diameter (ESD)) is about 18 μm .
21 | The number of grains per unit volume, N_V , (determined by N_{total}/V , where V is the
22 | gauge volume) is about $2.7 \times 10^{-5} \mu\text{m}^{-3}$ (see Table 1).
23 |

24 | Table 1. Microstructural parameters for recrystallized grains calculated based
25 | on DCT and EBSD data. V_V , D_{ESD} , N_V and N_{total} are volume fraction, average grain
26 | size, number of grains per unit volume and total grain number, respectively. For
27 | EBSD data, the D_{ESD} was calculated based on the statistical analysis.
28 |

	V_v	D_{ESD} (μm)	N_V ($10^{-5} \mu\text{m}^{-3}$)	N_{total}
DCT	24%	18.4	2.7	929
EBS	$28 \pm 4\%$	14.6	4.1	469

To verify the 3D results, the microstructure of the sample was characterized using a Zeiss Supra 35 field emission gun scanning electron microscope equipped with a Channel 5 EBSD system. EBSD measurements were conducted on the longitudinal section (defined by the RD and normal direction (ND)) using a scanning step size of $0.5 \mu\text{m}$, covering two areas of $\sim 6.7 \times 10^5 \mu\text{m}^2$.

An example of the EBSD maps is shown in Fig. 3a. The recrystallized grains are selected from the EBSD maps using the following criteria: i) grain size (equivalent circular diameter, ECD), larger than $3 \mu\text{m}$, ii) surrounded at least partly by high angle boundaries to the deformed matrix, iii) the internal misorientation angle is less than 1° . Fig. 3b shows the recrystallized grains only. Similar to the 3D results, clusters of recrystallized grains are seen in bands parallel to the RD. In total, 469 recrystallized grains are found. The V_v determined based on EBSD maps is slightly higher than that of the 3D result.

It should be noted that on the EBSD maps not all grains are sectioned through their maximum diameter; many grains appear smaller than they actually are, and large grains have a higher chance to be sectioned than small grains. A statistical analysis using stereology is required to link the 2D EBSD and 3D DCT data. In the present paper, the Schwartz-Saltykov (SS) method, which is a standard way to calculate 3D grain size (D_{ESD}) distribution based on the 2D size (D_{ECD}) distribution [19], is

1 performed to calculate the N_V and the average grain size (see the supplementary
2 materials).

3
4
5 The results show that the N_V determined from SS analysis is ~30% higher than
6 that from DCT data (see Table 1). In other words, ~30% of the recrystallized grains
7 are not seen in the DCT data set. To further understand the missing grains, the
8 distributions of N_V calculated from DCT and EBSD data are compared (see Fig. 4). It
9 is evident that the two distributions agree well to each other for the size range larger
10 than 10 μm , whereas DCT significantly underestimated the fraction of the small
11 grains ($<10 \mu\text{m}$). This comparison suggests that the low N_V of the DCT data is
12 primarily attributed to the small grains, which have been poorly indexed by DCT. As
13 a result, the average grain size determined based on the DCT data is larger than that
14 from the SS analysis, while the volume fraction of the recrystallized grains measured
15 from DCT data is slightly smaller than that from EBSD data (see Table 1).
16
17
18
19
20
21
22
23
24
25
26
27
28
29
30

31 The reason for the poor indexing of the small recrystallized grains is that the
32 small grains (especially in volumes) produce weak diffraction spots, which are
33 difficult to distinguish from the background noise and the diffused diffraction signal
34 from deformation matrix. As the intensities of diffraction spots from hkl families with
35 high numbers are much weaker than those with low numbers, identification of high
36 numbered hkl diffraction spots for even medium size grains (in the range 7-10 μm)
37 is a challenge. As a result, only a limited number of diffraction spots from low
38 numbered hkl families can be segmented properly, which is insufficient for indexing
39 and reconstructing the grains.
40
41
42
43
44
45
46
47
48
49
50
51
52

53 Despite the large number of the small recrystallized grains which are not
54 indexed by DCT, the volume fraction of those small grains is only less than 2% of the
55 total volume fraction of the recrystallized grains (see ~~in~~ Fig. 4). As recrystallization
56
57
58
59
60
61
62
63
64
65

1 proceeds and the nuclei/grains grow to large sizes and thus can be properly
2 reconstructed, this situation can be further remedied.
3

4
5 Compared with other 3D characterization techniques, such as 3DXRD [20-23]
6
7 and X-ray Laue microdiffraction [24,25], DCT has several advantages for
8
9 recrystallization studies. i) A large number of grains can be characterized
10
11 simultaneously, allowing a statistically-sound analysis, e.g. the 3D recrystallization
12
13 kinetics. ii) DCT provides fast measurements of reasonably large volumes (e.g.
14
15 $400 \times 400 \times 300 \mu\text{m}^3$). A typical DCT scan takes about 2 h. With the upcoming
16
17 synchrotron upgrade, the X-ray intensity can be improved by a factor of 40-100 [26].
18
19 With that implemented, both the spatial resolution (in term of the minimum detectable
20
21 grain size) and the temporal resolution can be improved significantly. In combination
22
23 with in-situ annealing, dynamic studies of recrystallization ~~studies~~ can be performed
24
25
26
27
28
29 in the near future.
30

31 32 33 **Acknowledgements:**

34
35
36 YBZ thanks Prof. D. Juul Jensen for the useful comments during the preparation of
37
38
39 the manuscript.
40

41 **References:**

- 42
43 [1] W. Xu, M.Z. Qadir, M. Ferry, Metall. Mater. Trans. A Phys. Metall. Mater.
44
45 Sci. 40 (2009) 1547–1556.
46
47
48 [2] G.H. Fan, Y.B. Zhang, J.H. Driver, D. Juul Jensen, Scr. Mater. 72–73 (2014)
49
50
51 9–12.
52
53 [3] Y. Zhang, D. Juul Jensen, Y. Zhang, F. Lin, Z. Zhang, Q. Liu, Scr. Mater. 67
54
55
56 (2012) 320–323.
57
58 [4] Z. Sükösd, K. Hannesson, G. Wu, D. Juul Jensen, 3rd Int. Conf. Recryst. Grain
59
60
61
62
63
64
65

Growth, *ReX GG III 558–559* (2007) 345–350.

- 1
2
3
4
5
6
7
8
9
10
11
12
13
14
15
16
17
18
19
20
21
22
23
24
25
26
27
28
29
30
31
32
33
34
35
36
37
38
39
40
41
42
43
44
45
46
47
48
49
50
51
52
53
54
55
56
57
58
59
60
61
62
63
64
65
- [5] H.F. Poulsen, W. Ludwig, E.M. Lauridsen, S. Schmidt, W. Pantleon, U. Olsen, J. Oddershede, P. Reischig, A. Lyckegaard, J. Wright, G. Vaughan, in: 31st *Risø Int. Symp. Mater. Sci.*, 2011, pp. 101–119.
- [6] H.F. Poulsen, *J. Appl. Crystallogr.* 45 (2012) 1084–1097.
- [7] D. Juul Jensen, H.F. Poulsen, *Mater. Charact.* 72 (2012) 1–7.
- [8] S. Schmidt, S.F. Nielsen, C. Gundlach, L. Margulies, X. Huang, D. Juul Jensen, *Science* 305 (2004) 229–32.
- [9] W. Ludwig, P. Reischig, A. King, M. Herbig, E.M. Lauridsen, G. Johnson, T.J. Marrow, J.Y. Buffière, *Rev. Sci. Instrum.* 80 (2009) 033905.
- [10] P. Reischig, A. King, L. Nervo, N. Viganó, Y. Guilhem, W.J. Palenstijn, K.J. Batenburg, M. Preuss, W. Ludwig, *J. Appl. Crystallogr.* 46 (2013) 297–311.
- [11] T.W. Cornelius, O. Thomas, *Prog. Mater. Sci.* 94 (2018) 384–434.
- [12] A. Yau, W. Cha, M. Kanan, G.B. Stephenson, A. Ulvestad, *Science* 356 (2017) 739–742.
- [13] B. Larson, W. Yang, G. Ice, J. Budai, J. Tischler, *Nature* 415 (2002) 887–890.
- [14] B.C. Larson, L.E. Levine, *J. Appl. Crystallogr.* 46 (2013) 153–164.
- [15] A. King, G. Johnson, D. Engelberg, W. Ludwig, J. Marrow, *Science* 321 (2008) 382–385.
- [16] J. Zhang, Y. Zhang, W. Ludwig, D. Rowenhorst, P.W. Voohees, H.F. Poulsen, *Acta Mater.* Accepted.
- [17] N. Viganò, W. Ludwig, K.J. Batenburg, *J. Appl. Crystallogr.* 47 (2014) 1826–1840.
- [18] N. Viganò, A. Tanguy, S. Hallais, A. Dimanov, M. Bornert, K.J. Batenburg, W. Ludwig, *Sci. Rep.* (2016) 20618.

- [19] E.E. Underwood, Quantitative Stereology., Addison-Wesley, 1970.
- [20] F.X. Lin, Y.B. Zhang, W. Pantleon, D. Juul Jensen, Philos. Mag. 95 (2015) 2427–2449.
- [21] S. Storm, D. Juul Jensen, Scr. Mater. 60 (2009) 477–480.
- [22] S.S. West, S. Schmidt, H.O. Sørensen, G. Winther, H.F. Poulsen, L. Margulies, C. Gundlach, D. Juul Jensen, Scr. Mater. 61 (2009) 875–878.
- [23] S. Van Boxel, S. Schmidt, W. Ludwig, Y.B. Zhang, D. Juul Jensen, W. Pantleon, Mater. Trans. 55 (2014) 128–136.
- [24] Y.B. Zhang, J.D. Budai, J.Z. Tischler, W. Liu, R. Xu, E.R. Homer, A. Godfrey, D. Juul Jensen, Sci. Rep. 7 (2017).
- [25] C. Xu, Y. Zhang, A. Godfrey, G. Wu, W. Liu, J.Z. Tischler, Q. Liu, D. Juul Jensen, Sci. Rep. 7 (2017) 42508.
- [26] ESRF upgrade programme phase II (2015-2019) white paper.

Figure captions:

Figure 1. A typical near-field diffraction image of the partially recrystallized Al sample, recorded using a near-field detector with 2048×2048 pixels (pixel size of 0.77 μm). The red arrows mark examples of diffraction spots originating from recrystallized grains, while the yellow ellipse marks diffraction from a deformed grain. The rectangle region in the middle is from the direct X-ray beam.

Figure 2. 3D reconstruction of recrystallized grains measured by DCT. (a) The 3D volume of $240 \times 420 \times 420 \mu\text{m}^3$; (b) a 2D section. The colors in both (a) and (b) represent the crystallographic orientation along RD (see the inset in (b)). In (b) thin

and thick black lines represent boundaries with misorientation $>2^\circ$ and $>15^\circ$,

respectively. The voxel/pixel size is $0.77 \mu\text{m}$.

Figure 3. Example of mMicrostructure of the partially recrystallized Al sample: (a)

full map, (b) recrystallized grains. The colors used in the EBSD maps correspond to

the crystallographic orientations along sample RD (see the inset in (b))direction. Thin

and thick black lines represent boundaries with misorientation $>2^\circ$ and $>15^\circ$,

respectively. The pixel size of the EBSD map is $0.5 \mu\text{m}$.

Figure 4. Distributions of grain size (D_{ESD}) and volume fraction ~~Size-(ESD)-distribution~~

of recrystallized grains determined based on EBSD and DCT data. The volume

fraction is calculated based on the distribution of N_V from the EBSD data using SS

method.

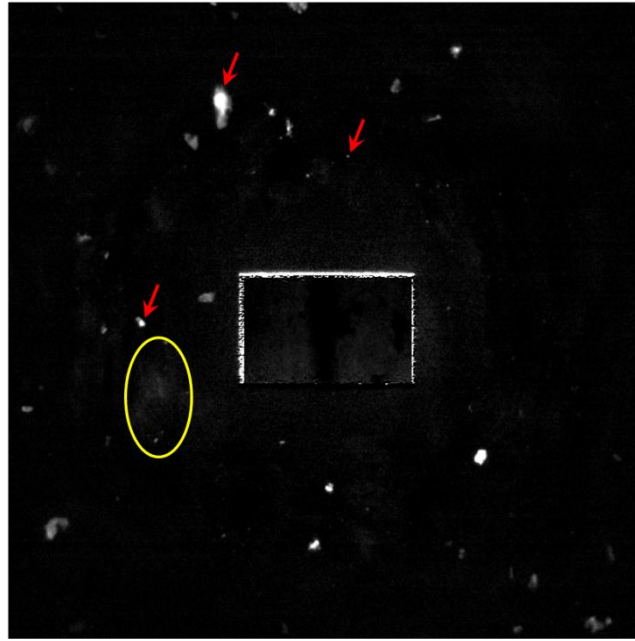


Figure 1. A typical near-field diffraction image of the partially recrystallized Al sample, recorded using a near-field detector with 2048×2048 pixels (pixel size of $0.77 \mu\text{m}$). The red arrows mark examples of diffraction spots originating from recrystallized grains, while the yellow ellipse marks diffraction from a deformed grain. The rectangle region in the middle is from the direct X-ray beam.

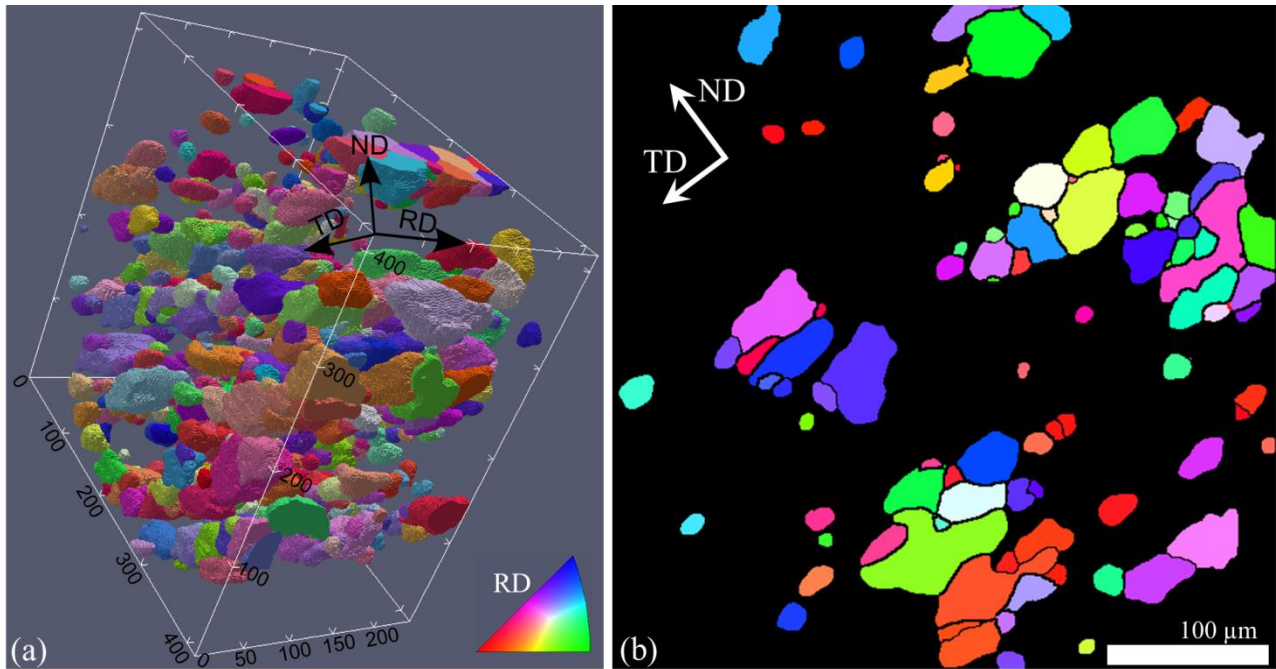


Figure 2. 3D reconstruction of recrystallized grains measured by DCT. (a) The 3D volume of $240 \times 420 \times 420 \mu\text{m}^3$; (b) a 2D section. The colors in both (a) and (b) represent the crystallographic orientation along RD (see the inset in (a)). In (b) thin and thick black lines represent boundaries with misorientation $>2^\circ$ and $>15^\circ$, respectively. The voxel/pixel size is $0.77 \mu\text{m}$.

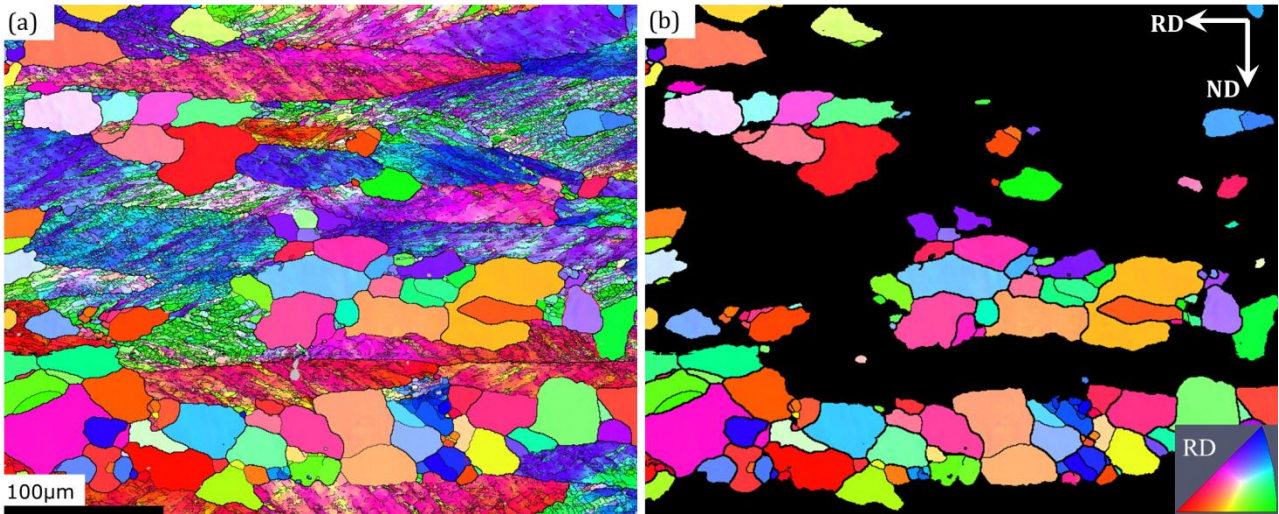


Figure 3. Example of microstructure of the partially recrystallized Al sample: (a) full map, (b) recrystallized grains. The colors used in the EBSD maps correspond to the crystallographic orientations along sample RD (see the inset in (b)). Thin and thick black lines represent boundaries with misorientation $>2^\circ$ and $>15^\circ$, respectively. The pixel size of the EBSD map is $0.5 \mu\text{m}$.

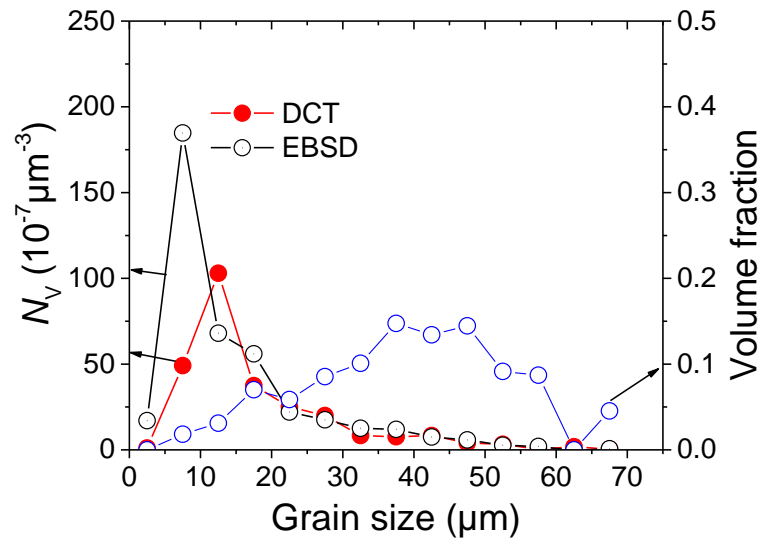


Figure 4. Distributions of grain size (D_{ESD}) and volume fraction of recrystallized grains determined based on EBSD and DCT data. The volume fraction is calculated based on the distribution of N_V from the EBSD data using the SS method.

Supplementary Material

[Click here to download Supplementary Material: supplementary materials.pdf](#)